



Hunukumbure, RMM., Beach, MA., Allen, B., Fletcher, PN., & Karlsson, P. (2001). *Smart antenna performance degradation due to grating lobes in FDD systems*. (pp. 5 p). <http://hdl.handle.net/1983/853>

Peer reviewed version

[Link to publication record in Explore Bristol Research](#)
PDF-document

University of Bristol - Explore Bristol Research

General rights

This document is made available in accordance with publisher policies. Please cite only the published version using the reference above. Full terms of use are available:
<http://www.bristol.ac.uk/red/research-policy/pure/user-guides/ebr-terms/>

Smart Antenna Performance Degradation due to Grating Lobes in FDD Systems

Mythri Hunukumbure⁽¹⁾, Mark Beach⁽¹⁾, Ben Allen⁽¹⁾, Paul Fletcher⁽¹⁾ & Peter Karlsson⁽²⁾

⁽¹⁾Centre for Communications Research,
University of Bristol, Quenen's Building, Bristol BS8 1TR, UK.
Tel: +44 (0) 117 928 8617, Fax : +44 (0) 117 954 5206
E-mail : Mythri.Hunukumbure@bris.ac.uk

⁽²⁾Telia Research AB, Malmo, Sweden.

ABSTRACT :

It is shown here that even for a small increase in the inter-element distance from the nominal half wavelength value, grating lobes could occur in smart antenna radiation patterns. This has practical implications when smart antennas are employed in Frequency Division Duplex (FDD) systems. This paper discusses the impact on the UMTS Terrestrial Radio Access (UTRA) FDD system. The presence of grating lobes is verified and the resultant performance degradation in an interference limited cell is quantified, using simulation results derived from actual field trial measurements taken within the UTRA band.

INTRODUCTION :

Within the 3rd generation wireless systems, there will be a much greater demand for system capacity, mainly due to the high data rate and multimedia services they promise to offer. Smart antennas are likely to play a significant role in meeting this need for capacity enhancement [1]. The radiation pattern of a smart antenna array is governed by the following factors -: radiation pattern of individual elements, number of elements, inter-element distance and amplitude/phase variations across the array. Usually the first three factors remain constant and the radiated power is optimised by the latter.

Due to the separation of up-link and down-link carrier frequencies in a FDD system, the inter-element separation as a function of wavelength will not remain constant. In certain cases, this can result in the generation of grating lobes within the same cell sector. If present, the grating lobes could capture additional interfering users, bringing down the carrier to interference ratio (C/I). Another implication would be the capturing of more multi-paths from the wanted user. Hence the occurrence of grating lobes would deteriorate the interference rejection capability of the smart antenna and also increase the multipath interference at the receiver.

This paper first analyses the conditions under which grating lobes would occur theoretically. Next an overview of the field trials is presented, which provided the data for the simulations. It is shown that within the field trials set up grating lobes would occur for some of the transmitting locations in smart antenna beam-forming. Finally the impact of the grating lobes is analysed in a simulated UTRA environment.

THEORETICAL ANALYSIS:

A radiation pattern generated by a uniform linear antenna array will contain complete grating lobes, if the following equation is satisfied for values other than $n=0$. [2]

$$\pi \cdot \frac{d}{\lambda} [\sin \theta_g - \sin \theta_0] = \pm n\pi \quad n=0,1,2 \dots \dots \dots (1)$$

θ_g = angular position of the Grating lobe in azimuth plane
 θ_0 = angular position of the main lobe in azimuth plane

d = inter-element distance
 λ = carrier wavelength

Assuming a tri sector cell, the maximum steering angle is $\pm 60^\circ$. i.e. $\theta_{0(\max)} = \pm 60^\circ$

$$\text{for } n=1, \quad \sin \theta_g = 0.8667 \pm \frac{\lambda}{d}$$

$$\text{in real space, } |\sin \theta_g| \leq 1, \quad \frac{\lambda}{d} \leq 1.8667 \quad \text{or} \quad d \geq 0.536 * \lambda \quad \dots\dots\dots(2)$$

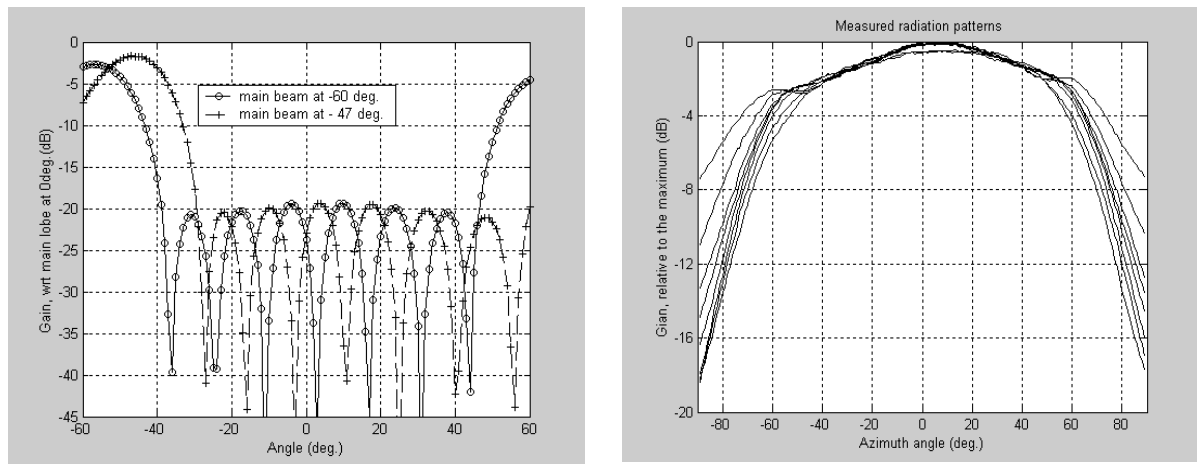
Thus, if the inter-element spacing is greater than 0.536 times the wavelength, grating lobes could occur within $-90^\circ < \theta_g < 90^\circ$ region when the main beam is steered towards $\theta_{0(\max)}$. Some of the energy in the grating lobe can spill into the operating cell sector, even if its apex is outside the $[-60^\circ \ 60^\circ]$ region.

The UTRA-FDD spectrum allocations provide a nominal 190MHz separation between the up-link and down-link carriers. Analysing the frequency allocation in UK [3] for example, it is evident that if $\lambda/2$ inter element spacing is employed on the up-link carrier, grating lobes will occur in down-link operation. Selecting the down-link carrier frequency for element spacing will reduce the electrical size of the array in the up-link, thus widening the main beam. Further there are practical design constraints in reducing the element separation.

THE FIELD TRAIL CAMPAIGN:

The following results are derived from data gathered through an extensive field trial campaign conducted in Bristol. Employing a state of the art channel sounder (Medav RUSK BRI) the channel was illuminated with a 20MHz multi-tone signal centred at 1920MHz, which was within the allocated frequency bands for UTRA. The channel response was received by an eight element antenna array and processed by the Medav receiver. Data logging across all elements was carried out within the coherence time of the channel. Further technical information on the field trails can be found in [4].

During post processing, the signal bandwidth was windowed to 5MHz, to comply with UTRA standards. The 1925-1930MHz sub-band was selected, which implies a carrier frequency at 1927.5MHz. The array was originally designed to operate in the 1800MHz GSM band with the physical element separation fixed to 85mm. This translates to 0.546λ at this carrier frequency. As the threshold ratio obtained in equation (2) is exceeded here, grating lobes can be expected in the operating cell sector. Figure (1) presents the radiation patterns in beam steering with the 8 element array, and calibrated element radiation patterns.



a) Radiation patterns from the 8 element array b) Individual element patterns (measured)

Figure (1) : Radiation patterns of the Smart antenna

Figure (1a) shows the presence of a significant spillage from a grating lobe in the operating sector, when the main beam is steered into -60° . Ideally the grating lobe should peak at 74.8° . The figure also shows

how the grating lobe spillage diminishes, when the main beam is steered to -47° . Similar results are implied at the opposite cell sector boundary. Amplitude weights derived from Dolph-Chebyshev technique have been incorporated, to achieve a 20dB side lobe reduction. Note that these radiation patterns within the cell sector slightly deviate from the ideal, due to the roll off effects in the individual element's radiation patterns as shown in figure (1b). Beyond the azimuth limits of the cell sector, the individual radiation patterns roll off sharply, so the grating lobes would not have significant effects on the adjacent sectors.

RESULTS :

In order to validate the presence of grating lobes, the signal powers received from five field trial locations were analysed. The transmitter was stationary during the 10s measurement periods. Smart antenna beam steering was carried out towards the dominant directions of signal arrival (DoA). To capture the signals from probable grating lobes, beam-forming was also carried out for the angles opposite to the dominant DoA's. Table (1) presents the results, i.e. the average received power and the dynamic range¹ of signal fluctuations for the above 2 cases.

User Location	Main beam at 'true' DoA			Main beam 'opposite to' DoA		
	Steering angle	Average Power (dBm)	Dynamic Range (dB)	Steering angle	Average Power (dBm)	Dynamic Range (dB)
A	60°	-18.58	3.25	-60°	-19.09	3.01
B	56°	-27.36	2.98	-56°	-27.71	2.88
C	24°	-36.40	3.16	-24°	-40.19	4.73
D	-60°	-16.47	1.01	60°	-16.77	0.84
E	-44°	-29.64	3.14	44°	-35.60	4.61

Table (1): Analysis of received signal power for different locations

Due to their DoA's, locations A, B and D were susceptible in generating grating lobes at the other end of the cell sector. The received signal parameters from these locations show a close similarity for the two opposing steering angles. Evidently the grating lobe components capture the signals from dominant DoA's when the main beam is at the opposing angles. The slight reductions in the average power and the dynamic range reflect the slightly lower gain and beam width of the grating lobe spillage. The DoA's for locations C and E are within the $[-47^\circ 47^\circ]$ range, so no grating lobe components will appear within the cell sector, in beam-forming. When the main beam is at the 'wrong' angle, the average received power for locations C and E, is considerably reduced as compared to locations A, B and D. For locations C and E, the main beam may still capture secondary multipath components and the side lobes will capture the dominant rays. The corresponding increase in the dynamic range for these locations suggests enhanced multipath activity.

Monte-Carlo simulations were conducted to investigate the capacity constraints the grating lobes could generate, in the presence of intra-cell interference. Data and control channels were modelled according to the UTRA-FDD physical layer specification [5], assuming a spreading factor of 32 for all users. This spreading factor implies a very high data rate (120kb/s) for the users. Perfect knowledge of the channels was assumed and power control was introduced at the receiver to eliminate 'Near-Far' effects. Channel responses at the receiver were gathered after beam forming towards the DoA of the single wanted user. A fixed level of additive white Gaussian noise was added to the channels to give a signal to noise ratio of 10dB. Figure (2) shows the results of bit error rate vs. the number of interfering users, for 2 locations of the wanted user.

¹ Defined as the ratio of maximum to minimum instantaneous received power

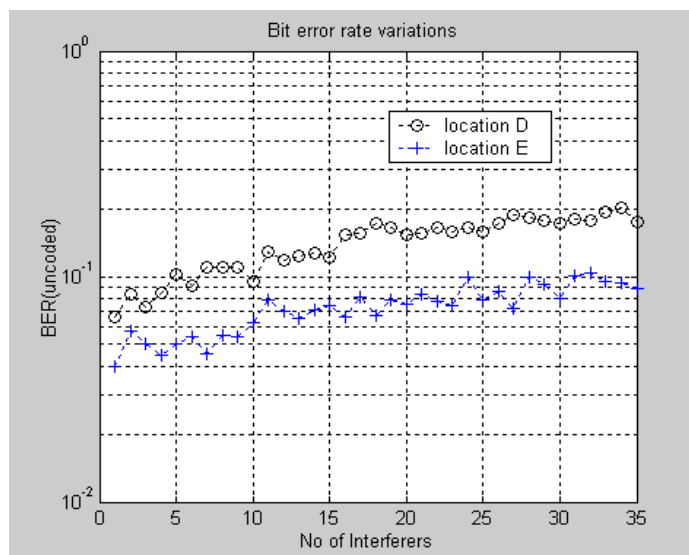


Figure (2) : BER vs Interference for two user locations

As discussed above, beam-steering towards location D causes a grating lobe within the cell sector. The increased BER for location D suggests that the grating lobe captures significant levels of additional interference. On average, the BER for location D has increased by 0.068, which accounts for a 93% degradation from values obtained for location E. It should be noted that if an error correction coding scheme was incorporated, both BER curves would improve by a factor of 10^{-2} . The same set of users (uniformly spread across the cell) was considered in both cases, except for the swapping of the wanted user. Hence this performance degradation can be attributed to the formation of grating lobes.

CONCLUSIONS:

It is shown that grating lobes can occur in FDD systems and they would degrade the spatial filtering capability of a smart antenna receiver. The effects of grating lobes are presented in the form of a BER degradation, in an interference limited cell. In UTRA FDD systems, the occurrence of grating lobes will result in a significant capacity reduction.

REFERENCES:

- 1) M. Beach, C. Simmonds, P. Howard, P. Darwood, "Smart Antennas : an enabling technology for the wireless revolution" Conference proceedings, AP 2000, Davos, Switzerland.
- 2) M.I. Skolnik, 'Introduction to Radar systems' (1980,second edition) Published by McGraw Hill. Chapter 8, pp. 283.
- 3) S. Deghan, D. Lister, R. Owen, P. Jones , "W-CDMA Capacity and planning issues" IEE Electronics and Communications Engineering Journal, June 2000, pp101-118
- 4) M. Beach, B. Allen, P. Karlsson, "Correlation of Power Azimuth Spectrum for varying Frequency Division Duplex spacings", Conference proceedings EPMCC 2001, Vienna, Austria.
- 5) 3GPP Technical specification : 3G TS 25.213. V3 1.1
(Under the official web site of the 3rd Generation Partnership Project – <http://www.3GPP.org>)

ACKNOWLEDGEMENTS:

The authors wish to gratefully acknowledge the funding support under HEFCE JREI'98 which enabled the procurement of Medav channel sounder and Allgon systems AB, for providing the antenna array. They also thank Darren McNamara (affiliated to CCR, university of Bristol) for his helpful comments.

